Clays and Clay Minerals, Vol. 69, No. 1:52–67, 2021

CLAY MINERALOGY OF SURFACE SEDIMENTS IN THE THREE GORGES RESERVOIR: IMPLICATIONS FOR SEDIMENT PROVENANCES AND WEATHERING REGIMES

Shuai Wang[1], Wenbo Rao[1]*, Jin Qian[2], Mengying He[3], Changping Mao[1], Kun Li[2], Yuexing Feng[4], and Jianxin Zhao[4]

[1]College of Earth Sciences and Engineering, Jiangning Campus of Hohai University, Nanjing 211100, China
[2]College of Environment, Gulou Campus of Hohai University, Nanjing 210098, China
[3]School of Geography Science, Nanjing Normal University, Nanjing 210046, China
[4]Radiogenic Isotope Facility, The University of Queensland, Brisbane, QLD 4072, Australia

Abstract—Knowledge of clay mineralogy is essential for understanding the source areas and weathering environments of fluvial sediments, particularly in large reservoirs facing serious problems with sediment deposition, such as the Three Gorges Reservoir (TGR) in east-central China. The purpose of the present study was to identify the sediment provenances and weathering regimes contributing to the sediment load in the TGR by determining the clay-mineral and geochemical compositions of surface sediments during various seasons. X-ray diffractometry and scanning electron microscopy (SEM) were used to identify the clay minerals. The results showed that illite was the dominant mineral, followed in order by kaolinite, chlorite, and montmorillonite. From a mineralogical perspective, distal sources were the main contributors to the TGR sediments, and regional sources (surrounding tributaries) also contributed much during the three seasons, while proximal sources (hillslope soils) supplied sediment in the flood season but not in the other two seasons. The geochemical and hydrological data generally supported the mineralogical results. In the flood season, the chemical indices of the TGR sediments were >0.4, showing that the sediments contained Al-rich illite minerals and experienced intense hydrolysis. In the other two seasons the TGR sediments were enriched in Fe- and Mg-rich illite minerals, resulting from strong physical weathering. Furthermore, precipitation, rather than air temperature or latitude, was the factor that controlled weathering intensity. These findings provide deep insights into the sediment cycle and chemical weathering in this large reservoir basin.

Keywords—Chemical weathering · Clay minerals · Provenance identification · Surface sediment · Three Gorges Reservoir

INTRODUCTION

The Three Gorges Reservoir (TGR) is the world's largest hydropower project and the most important water conservancy regulation scheme. The total water storage capacity and the flood regulation capacity of this reservoir are 39.3 km^3 and 22.1 km^3, respectively, enabling hydropower generation, disaster reduction, and navigation improvement (Fu et al. 2010; Zhang and Lou 2011). The impoundment of the Three Gorges Reservoir caused a great number of environmental problems, however, most of which were related to sediment deposition (Wu et al. 2003; Xu et al. 2013a).

Sediment deposition has affected river processes in navigation channels and ports in backwaters, as well as the smooth operation of power plants and navigation gates. Due to the deposition of sediment in the TGR, the sediment concentration in the water flowing downstream has been greatly reduced, which increased the scouring of the downstream riverbed by the current, resulting in a lowering of the water level and further affecting inland navigation. At the same time, sediments are the main carriers of pollutants such as nutrients and heavy metals, thus promoting the development of eutrophication of the TGR aquatic ecosystem (Xu et al. 2013a). The sediment accumulation was estimated to be 1.67×10^9 tons with a mean deposition flux of ~1.11×10^8 ton/y in the TGR during 2003–2017 according to the Yangtze River Sediment Bulletin (CWRC 2003–2017). At present, dredging sediments is a popular way to inhibit the rapid increase in sediment deposition in this reservoir (Li et al. 2011). The most effective approach, however, is to prevent soil erosion in the source areas to avoid excessive sediment deposition in the TGR. Identifying the provenance of reservoir sediments is essential, therefore, to establish connections between sources and sinks, to focus on reducing sediment deposition by larger contributors, and to effectively solve the problem of sedimentation in the TGR.

Since the TGR commenced operation in 2003, many studies have examined the sediment provenance and weathering regimes in the TGR and in the Yangtze River (CWRC 2003–2017; Yang et al. 2007, 2014; Chen et al. 2008; He et al. 2013; Zhao et al. 2018). For example, CWRC (2003–2017) calculated the sediment inflow from upstream tributaries but excluded the sediments derived from the ungauged areas within the TGR watershed. The ungauged areas were taken into account by Yang et al. (2007) and Chen et al. (2008) but they assumed that the ratio of ungauged sediment inflow to gauged sediment inflow remained stable. The ungauged sediment discharge was estimated separately by Yang et al. (2014); their calculation was based on the assumption that larger sediment discharge from sources led to greater sediment deposition in the

* E-mail address of corresponding author: raowenbo@163.com
DOI: 10.1007/s42860-020-00106-5

TGR, however, and did not consider the sediment transported downstream. These studies were calculated based on hydrological data only; other methods should also be applied to determine the sources accurately. Several studies have attempted to decipher the sediment provenance and weathering regime by clay mineralogy in the Yangtze River but have rarely focused on the TGR (He et al. 2013; Zhao et al. 2018).

As important constituents of fine-grained sediments, clay minerals are widely distributed in fluvial and marine sediments (Gingele et al. 2001; Guyot et al. 2007; Liu et al. 2007; Adriaens et al. 2018; Khan et al. 2019). Clay mineral assemblages are sensitive to source-rock geology and chemical weathering and are considered to be effective indicators of the characteristics of the source areas; when they are entrained in a water mass, they can be transported over considerable distances from their source areas (He et al. 2013; Liu et al. 2018; Zhao et al. 2018). Illite and chlorite usually reflect a dry-cold climate and/or low rainfall (Winkler et al. 2002; Pang et al. 2018). In contrast, kaolinite forms mainly due to pedogenesis, which is characterized by strong hydrolysis and complete removal of mobile cations (Vanderaveroet 2000; Pang et al. 2018). A high concentration of kaolinite implies a typically warm-humid climate. Montmorillonite forms in the early weathering process of unstable Fe-, Mg-, and Ca-rich minerals, which are contained in igneous or metamorphic rocks and distributed in temperate and cool climate zones characterized by moderate hydrolysis (Liu et al. 2010; He et al. 2013). In a hot and humid climate, montmorillonite is destroyed in the process of soil formation (Liu et al. 2010; He et al. 2013). Clay mineralogy can reveal the driving factors of weathering and clarify more recent trends in the climate and weathering conditions in the source areas (Wang et al. 2016; Khan et al. 2019). In summary, clay minerals can be regarded as useful tools for identifying sediment provenances, transport patterns, and weathering regimes in a basin. Major and trace-element compositions of fluvial sediments are controlled by weathering, lithologies, diagenesis, and sedimentary sorting and can also be used to identify geochemical processes and provenance of clastic materials (Yang et al. 2004; Yang and Youn 2007; Rao et al. 2015).

The work presented here is a comprehensive and coordinated study of mineralogical and geochemical data for sediments from the main stream and tributaries and soils from hillslopes in the TGR basin to understand: (1) the clay-mineral assemblages and geochemistry of sediments in the TGR; (2) the provenance of sediments during different seasons; and (3) the nature and extent of weathering in the catchment of the TGR. The present study provides a good example of studies in the field of clay science in China and adds to the significance of clay research (Zhou et al. 2016).

STUDY AREA

The TGR extends 663 km from Yichang to Chongqing along the main stream of the Yangtze River, with a total water surface area of ~1080 km^2 (Fig. 1). The TGR was gradually impounded with phased increases in the water level to 135 m, 156 m, and 175 m in 2003, 2006, and 2010, respectively (Lu and Higgitt 2001; Bao et al. 2015). Since the impoundment behind the Three Gorges Dam (TGD), the water level has fluctuated between 145 m and 175 m, which interrupts the natural balance of sediment transport from the upper to lower reaches of the Yangtze River. The TGR operation is characterized by anti-seasonal water level changes; i.e. a high water level is maintained in the dry season, but a low water level is maintained in the flood season.

The Three Gorges Dam intercepts the main channel of the Yangtze River at the outlet of its upper subbasin and controls a drainage area of ~1×10^6 km^2 (Fig. 1) which produces major quantities of water and sediment (Yang et al. 2002). The sediment deposition flux shows a decreasing trend in the TGR (CWRC 2003–2017; Huang et al. 2019). Cascade dams such as Xiangjiaba, Xiluodu, Baihetan, and Wudongde will be located in the lower reaches of the Jinshajiang River; these dams are under construction or will be built on the main stream and tributaries of the upper Yangtze River. They may play an important role in reducing sediment transport and alleviating sediment deposition in the Three Gorges Reservoir. On the other hand, the continuous implementation of soil and water conservation and reforestation measures advocated by governments will help to reduce the suspended sediment flux in the Yangtze River (Tang et al. 2016).

The TGR basin has a monsoonal climate with annual mean air temperature and precipitation of 17–19°C and 1000–1200 mm, respectively. The winter is cold with an average temperature of 10°C and the summer is hot with an average temperature of 28–30°C (CNEMC 1997–2017). June to September is regarded as the flood season, while November to February is considered the dry season, and other months are known as the even season (Lou and Yin 2016). A large fraction of the annual precipitation occurs from June to September (Xu et al. 2010). Soils are developed mainly based on weathered rocks in this basin (Bao et al. 2015).

Tectonically, the TGR basin lies in the Yangtze Craton (Fig. 1c). This region is characterized by arrays of rolling hills and valleys. Clastic and carbonate rocks are distributed extensively with sporadic outcrops of magmatic and metamorphic rocks in this basin. Two different subregions are distinguished based on regional landforms and geology in this basin (Fig. 1). The upper-middle section is dominated by a hilly landscape and underlain by purple and red rocks composed of sandstone and mudstone. The lower section is a mountainous landscape with high mountains and deeply incised channels, and carbonate rocks comprise limestone and dolomite (Bao et al. 2015).

The Yangtze River flows mostly among Mesozoic and Cenozoic rocks in the upper part of the Yangtze River Basin, which are underlain by Upper Paleozoic rocks. The upper basin consists of meta-igneous rocks and meta-sedimentary rocks, carbonate rocks, and igneous rocks, especially Himalayan intermediate-felsic igneous rocks. The middle-lower basins are composed mainly of Paleozoic marine and Quaternary fluviolacustrine sedimentary rocks, intermediate-felsic igneous

https://doi.org/10.1007/s42860-020-00106-5 Published online by Cambridge University Press

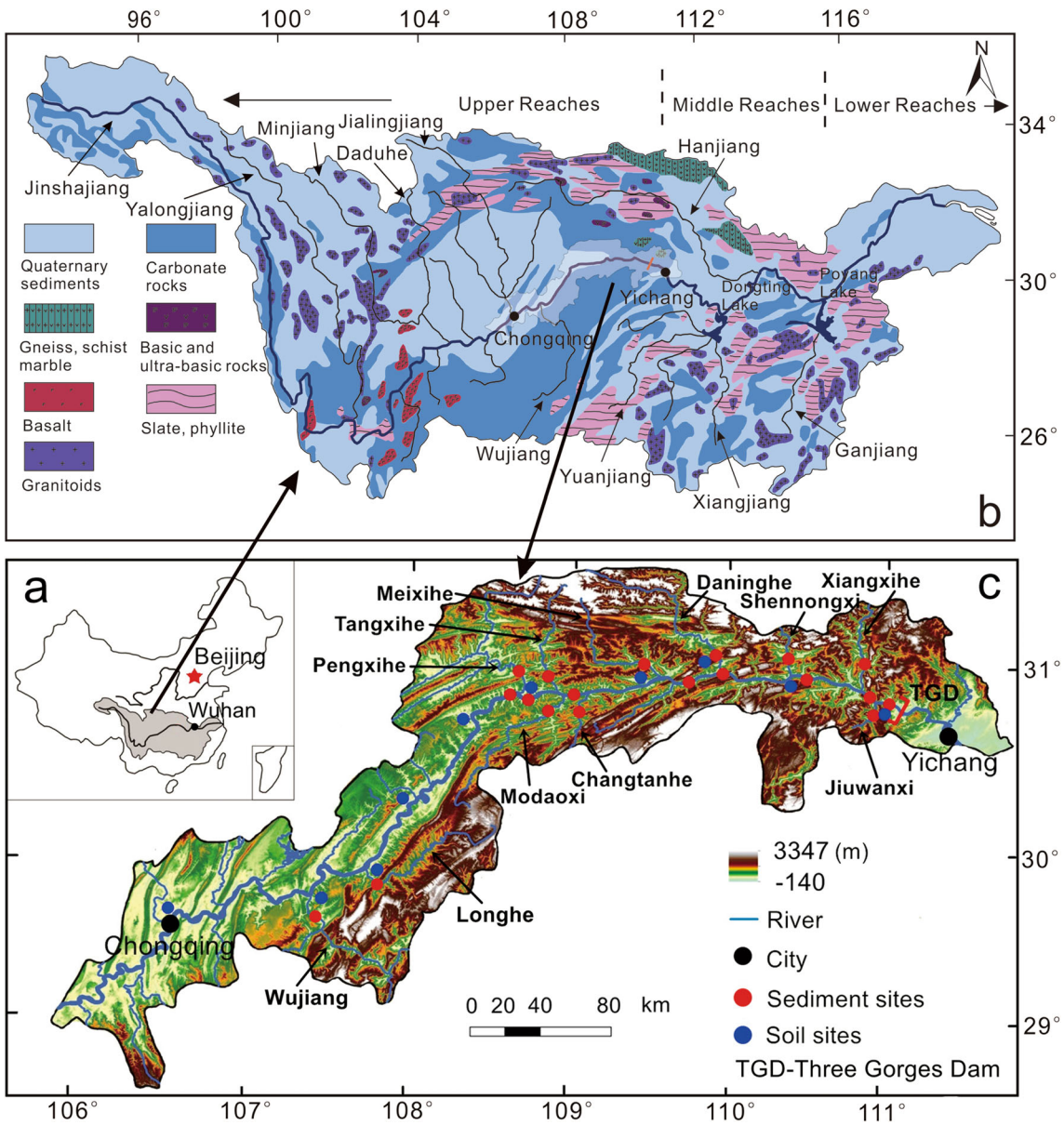

Fig. 1 Sketch map showing **a** the Yangtze River Basin, **b** Yangtze River major tributaries and main rock types, modified from Yang et al. (2009), and **c** the Three Gorges Reservoir and sampling sites

rocks and ancient metamorphic rocks. Various tributary basins are composed of different source-rock types from various tectonic settings (Fig. 1).

SAMPLES AND METHODS

Field Sampling

Surface sediment samples were collected from the top 5 cm of the sediment columns with a stratified sampler (DT-101B, Weifang, Shandong, China) onboard a ship in the Three Gorges Reservoir in July and December 2017 and in April 2018, except for the two samples from Wujiang and Longhe which were collected in April 2018 (Fig. 1). The hillslope soil samples in the TGR were collected during April 2018. All soil samples were obtained from the surface layer of 10 cm, and large dead leaves and stones were removed. These soils were mixed evenly and placed in polyethylene self-sealing bags for preservation. In total, the samples consisted of 53 surface sediment samples and ten soil samples. Each sample was treated as follows for mineralogical and chemical analyses. The <63 μm fraction was separated from the bulk sample by wet sieving and chosen as the study target, and this fraction was further treated at room temperature with 10% H_2O_2 (Hushi, Shanghai, China) for 48 h and 1 mol/L acetic acid (Hushi, Shanghai, China) for 24 h to remove organic matter,

https://doi.org/10.1007/s42860-020-00106-5 Published online by Cambridge University Press

secondary carbonates, and adsorbed contaminants. Finally, the treated fraction was washed with ultrapure water, centrifuged, dried at 105°C in an oven (DUG-9240A, Shanghai, China), and powdered in an agate mortar. Physical and chemical pretreatments were performed to obtain provenance signals from the given grain-size residual fraction that were not affected by particle sorting and post-depositional processes (Rao et al. 2015).

Analytical Methods

First, organic matter and secondary carbonate were removed from bulk samples using 10% H_2O_2 and 0.1 mol/L HCl (Hushi, Shanghai, China). Then, the samples were fully dispersed by the addition of sodium hexametaphosphate $(NaPO_3)_6$ (Hushi, Shanghai, China). After this step, the grain-size measurements were performed using a laser diffraction particle analyzer (Mastersizer-2000, Cambridge, UK) at the Institute of Surficial Geochemistry, Nanjing University, China. The relative error was ~3% according to duplicate determinations.

Major elements were determined by X-ray fluorescence using an ARL 9800 spectrometer (Boston, Massachusetts, USA) at the Center of Modern Analysis, Nanjing University, China. The 0.6 g sample was mixed thoroughly with 6.6 g of the fluxing agents Li tetraborate (Kermel, Tianjin, China) and Li metaborate (Tianjin, China) ($Li_2B_4O_7/LiBO_2$ = 67/33) and 0.6 mL of 40 mg/mL of LiBr in a Pt-Au crucible (Tianjin, China). The mixture was fused using an automatic gas-fired CLAISSE burner system (M4, Panalytical, Beijing, China) to make a glass disc for XRF measurement. Work curves were established on the basis of the national geological standard samples (GBW07401–GBW07408, GBW07301–GBW07312, and GBW07103–GBW07108). Major-element concentrations were expressed as oxide concentrations from the output of instrumental measurements. The absolute errors were <±0.5% and <±0.3% for SiO_2 and Al_2O_3, respectively. The relative errors were <5% for CaO, K_2O, Fe_2O_3, and TiO_2 and <10% for MgO, Na_2O, P_2O_5, and MnO.

Trace element analysis was performed using an Agilent-7500a (Santa Clara, California, USA) inductively coupled plasma mass spectrometer (ICP-MS) at the University of Queensland (RIF-UQ), Australia. Each sample was dissolved in an acid mix (1:1) of distilled HF (Ajax Finechem, Melbourne, Victoria, Australia) and HNO_3 (Ajax Finechem, Melbourne, Victoria, Australia) in a high-pressure jacket equipped with a Teflon beaker in an oven for 48 h to ensure complete digestion/dissolution. This procedure was repeated using larger amounts of acids for an additional 24 h. After digestion, the sample was evaporated to incipient dryness, refluxed with 6 N HNO_3, and heated again to incipient dryness. The sample was then dissolved in 2 mL of 3 N HNO_3 and diluted with Milli-Q water (18 MΩ cm) to a final dilution factor of 2000. The rock standards GSR-1, GSR-3, and AGV-2 were used to monitor the analytical accuracy and precision. The analytical accuracy, as indicated by the relative difference between the measured and recommended values, was better than 5%.

Scanning electron microscopy (SEM) analysis was performed using a Hitachi S-3400N (Tokyo, Honshu, Japan) instrument at the Center of Modern Analysis, Nanjing University, China. Representative bulk samples were prepared for SEM-EDX analysis by adhering the fresh broken surface of each rock sample using double-stick tape to an aluminum sample holder and coating the surface with a thin film of gold using a Giko ion coater (Hitachi E-1010, Tokyo, Honshu, Japan). The mineral composition of the <63 μm residual sample was determined qualitatively with an ARL-X'TRA (Boston, Massachusetts, USA) powder X-ray diffractometer with CuKα radiation, a voltage of 40 kV, a current of 40 mA, and continuous scans of 3–65°2θ at the Center of Modern Analysis, Nanjing University, China. Semi-quantitative estimates of relative mineral percentages were obtained from Cook et al. (1975). The terms quartz, plagioclase, K-feldspar, and clay minerals were used here as general expressions for the respective mineral groups.

The clay fraction was separated from the bulk sample based on Stokes's law, suspended in deionized water, and allowed to dry on glass slides to form oriented aggregates after removal of carbonate and organic matter. Then, the clay fraction was air dried, solvated for 12 h over a closed drying container with ethylene glycol (EG) in the bottom, covered by a lid coated with vacuum silicone grease in an oven at 60°C, then analyzed by XRD. This sample was heated to 550°C for 2 h and analyzed again by XRD. The XRD analyses were carried out using an X'TRA (Boston, Massachusetts, USA) X-ray diffractometer (Ni-filtered CuKα radiation, 40 kV voltage, and 40 mA current) with an error of <8% at the Center of Modern Analysis, Nanjing University, China. The clay slides were scanned from 3 to 35°2θ with a step size of 0.02°2θ. All clay minerals were identified and their peak areas obtained using the *JADE* software (Zhao et al. 2018). The terms montmorillonite, illite, kaolinite, and chlorite are used here as general expressions for the respective clay mineral groups. Semi-quantitative estimates of relative clay mineral percentages were obtained from measurements of XRD pattern peak areas, which were multiplied by the weighting factors from Biscaye (1965), namely, four times the illite peak area, two times the kaolinite + chlorite peak area, and one times the montmorillonite peak area, and then normalized to 100%. The relative proportions of kaolinite and chlorite were determined on the basis of the ratio of the 3.57/3.54 Å peak areas. Clay minerals were identified according to the position of the (001) series of basal reflections on the XRD patterns of air-dried, ethylene-glycolated, and heat-treated specimens. Illite was identified by the basal 10 Å peak; this basal spacing remained unaffected after the glycolation and heating treatments (Fig. 2). Kaolinite was recognized by its 7 Å peak, which disappeared after heating to 550°C. Montmorillonite exhibited a broad 12–15 Å reflection which increased to 17 Å after saturation with ethylene glycol. Chlorite was characterized by a first-order peak at 14 Å and a third-order peak at 4.7 Å, which did not expand when glycolated. After heating to 550°C, the 14 Å reflection was enhanced and shifted its position to 13.8 Å (Fig. 2).

Illite crystallinity was obtained from the half-height width of the 10 Å peak. Lower values represent greater crystallinity, characteristic of weak hydrolysis of continental source rocks

https://doi.org/10.1007/s42860-020-00106-5 Published online by Cambridge University Press

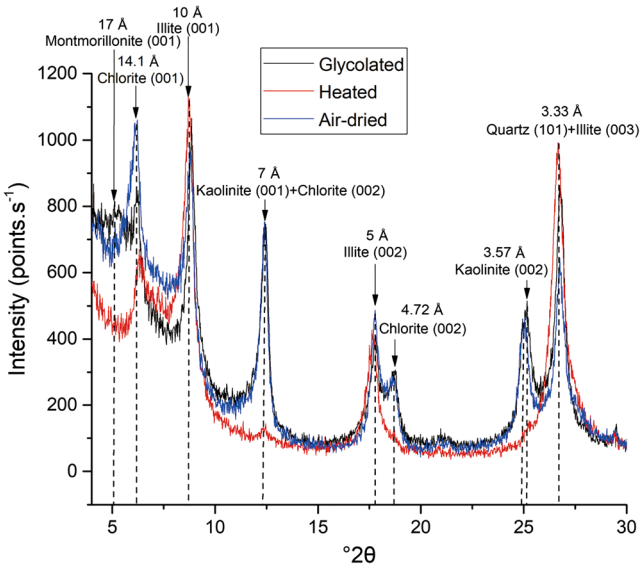

Fig. 2 XRD traces of clay minerals in the TGR

and arid/cold climatic conditions (Chamley 1989; Ehrmann 1998). This index was also used as a potential tracer of source regions and transport paths. The illite chemistry index, which can mirror the weathering regime of the sediment provenance (Ehrmann 1998; Liu et al. 2003), refers to the ratio of the 5 and 10 Å peak areas. Ratios <0.5 represent Fe-Mg-rich illites (biotite micas), implying physical erosion; ratios >0.5 are found in Al-rich illites (muscovites), indicating strong hydrolysis (Gingele et al. 2001; Liu et al. 2008).

Data Analysis

One-way ANOVA was used to identify significant differences in clay mineral assemblages of the sediments during different seasons. The statistical analysis was performed with the IBM *SPSS Statistics* 22 software. All graphics were developed with the *Origin* 2016 software.

RESULTS AND DISCUSSION

Grain Size, Mineral Composition, and Scanning Electron Microscopy

The main stream sediments were composed mainly of clay and silt with little sand (Supplementary Material Fig. S1). The clay (<4 μm) and silt (4–63 μm) fractions ranged from 17.8 to 39.4% and from 59.9 to 76.9%, respectively. The sand fraction (>63 μm) comprised <5% in most sediment samples. The main stream sediment had a regular grain-size variation with season (Fig. S1), i.e. the sediment was coarser during the even season, finer during the flood season, and intermediate during the dry season in the TGR.

Qualitative XRD analyses showed that common minerals were dominated by quartz, followed by clay minerals, plagioclase, and K-feldspar in the TGR sediments and hillslope soils (Fig. S2). The relative content of quartz was >50% in TGR main stream sediments throughout the three seasons and was >60% in TGR tributary sediments and hillslope soils (Table S1). The relative clay mineral content was ~20% in sediments and hillslope soils of the TGR. The plagioclase and K-feldspar contents were 13.3 and 8.4%, respectively, in sediments and hillslope soils of the TGR (Supplementary Material Table S1). Carbonate minerals were not detected by XRD, as a result of acid pretreatment.

The TGR sediments and hillslope soils were rich in clay minerals as revealed by SEM analysis (Fig. 3a). Fine-grained samples were coated with irregular flaky smectite and scaly illite (Gürel and Özcan 2016; Gürel 2017). Books of kaolinite and leaf-shaped chlorite were also found in TGR sediments and soils (Fig. 3b,c). Moreover, honeycomb- or cotton-like mixed layers of illite-montmorillonite were scarcely present in the TGR sediments and soils (Fig. 3d).

Geochemical Characteristics of TGR Sediments, Hillslope Soils, and Basement Rocks

Major and trace-element analyses of the TGR sediments and hillslope soils during the flood, dry, and even seasons (Table 2) revealed large concentrations of SiO_2 and Al_2O_3 and small amounts of other elements. SiO_2 and Al_2O_3 accounted for ~80% of the composition of individual samples, supporting the mineralogical results. The TGR main stream sediments showed larger amounts of Al_2O_3, Fe_2O_3, Cu, and Pb and smaller amounts of SiO_2, Zr, and U than those of the tributary sediments and hillslope soils. Mean elemental concentrations did not differ greatly among the three seasons for the TGR sediments (Table 2). In addition, Wang et al. (2018) reported that the major and trace element contents of basement rocks were lower than those of the sediments and soils in the TGR, especially Fe, Mg, Mn, P, Ti, V, Cr, Co, Ni, Cu, Zn, and Sc. The K, Na, Rb, Zr, Nb, and Hf contents in the basement rocks were slightly larger than those of the sediments and soils in the TGR, however (Fig. 4). The UCC-normalized patterns of the TGR sediments were roughly similar, especially in the major element section

https://doi.org/10.1007/s42860-020-00106-5 Published online by Cambridge University Press

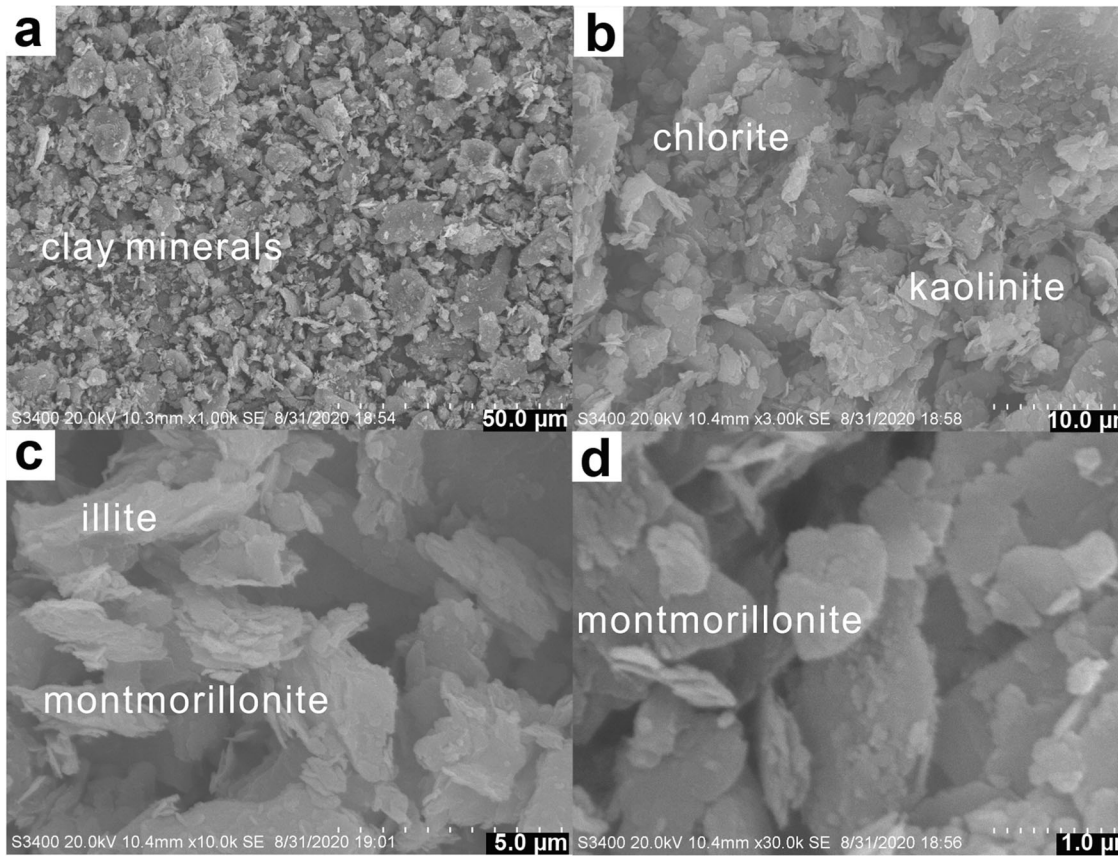

Fig. 3 SEM images showing the sediment characteristics of the TGR

(Fig. 4). Relative to the UCC (Taylor and McLennan 1985), TGR sediments and soil were enriched in Al_2O_3, Fe_2O_3, MgO, MnO, TiO_2, Li, Cu, Zn, Nb, and Pb and partly in Ba, Sc, and some high field strength elements (Y, Zr, Nb, Pb, and Th) but depleted in other elements. While the basement rocks were distinctly depleted in Ca, Fe, Mg, Mn, P, and some metallic elements, other elements showed contents equivalent to those of the UCC (Fig. 4).

Clay-Mineral Compositions in the TGR Sediments

The clay-mineral assemblages of the main stream sediments were dominated by illite (65.7–80.6%), with an average of 74.7%. Kaolinite (8.9–16.9%) and chlorite (4.6–16.9%) were less abundant, with average contents of 12.5 and 9.5%, respectively. Montmorillonite (0.2–7.5%) was scarce, with a mean of 3.4% in the TGR main stream (Table 1). The illite chemical index ranged from 0.29 to 0.55 with a mean of 0.43, and the illite crystallinity values were in the range 0.44–0.60°Δ2θ with an average of 0.52°Δ2θ (Table 1).

The clay-mineral assemblages showed no significant differences among the three seasons (ANOVA, P>0.05) (Fig. 5). On average, the illite and kaolinite contents in the flood season (72.5 and 12.0%, respectively) were slightly smaller than those in the dry and even seasons (75.6 and 12.4%; 75.9 and 13.1%, respectively). The chlorite and montmorillonite contents in the flood season (average 10.9% and 4.7%, respectively) were slightly greater than those in the dry season and even season (averages 9.1 and 2.9%; 8.4 and 2.6%, respectively). The clay mineral assemblages did not show regular trends along the water-flow direction in the main stream sediments, however (Fig. 5).

In addition to the main stream sediments, those of the TGR tributaries had clay-mineral assemblages that were dominated by illite (58.0–85.3%), with an average of 75.4% (Table 1). Kaolinite (4.2–17.9%) and chlorite (1.7–16.4%) were less abundant, with average contents of 10.6% and 9.5%, respectively (Table 1). Montmorillonite (0.4–11.2%) was scarce, with a mean of 4.6% in the TGR tributaries (Table 1). The clay-mineral contents in tributary sediments were equivalent to those in main stream sediments. The illite chemical index varied between 0.20 and 0.58 with a mean of 0.39 (Table 1); the illite crystallinity value ranged from 0.46–0.65°Δ2θ with an average of 0.52°Δ2θ (Table 1).

As shown in Fig. 6, the clay-mineral assemblages of each tributary river showed no obvious seasonal variations (ANOVA, P>0.05). On average, the montmorillonite and kaolinite contents in Xiangxihe were greatest, with means of 8.2 and 16.5%, respectively. The illite content in Meixihe was the largest, with a mean of 82.4%. The chlorite content in Changtanhe was greatest, with an average of 12.7%. The montmorillonite contents of the TGR tributaries were equivalent to those of upstream tributaries on the TGR except for

https://doi.org/10.1007/s42860-020-00106-5 Published online by Cambridge University Press

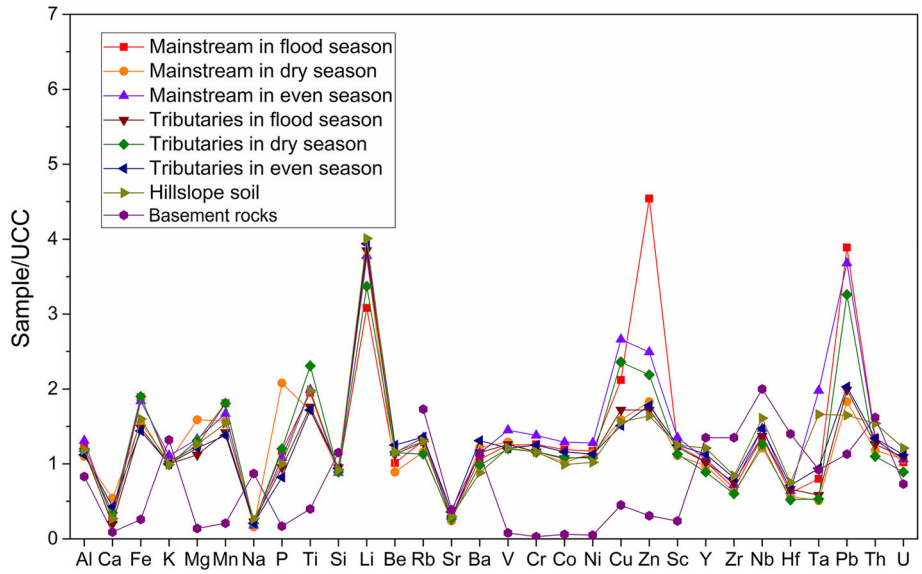

Fig. 4 UCC-normalized patterns of major and trace elements in sediments, hillslope soil, and basement rocks of the TGR. The data for basement rocks are from Wang et al. (2018)

Jialingjiang (Fig. 6). The kaolinite contents of the TGR tributaries were greater than those of Daduhe but less than those of Yalongjiang. The chlorite contents of the TGR tributaries were generally less than those of the upstream tributaries (He et al. 2013).

The clay mineral assemblages of the TGR hillslope soils were dominated by illite (58.9–84.9%), with an average of 69.9%, less than those of main stream and tributary sediments on average (Table 1). Kaolinite (2.8–19.0%) and chlorite (8.3–25.6%) were less abundant, with average contents of 9.0 and 15.2%, respectively (Table 1). The kaolinite contents of the hillslope soils were close to those of main stream and tributary sediments, but the chlorite contents of the hillslope soils were much higher than those of main stream and tributary sediments (Table 1). Montmorillonite (2.1–11.5%) was scarce with a mean of 5.8% in the TGR hillslope soils, slightly higher than those of main stream and tributary sediments (Table 1). The illite chemical index was between 0.18 and 0.53 with a mean of 0.38, and the illite crystallinity value ranged over 0.33–0.72°Δ2θ with an average of 0.52°Δ2θ (Table 1). The illite chemical indices and the illite crystallinity values were similar in the main stream and tributary sediments and the hillslope soils (Table 1).

Clay minerals in the hillslope soils showed an obvious spatial trend from upstream to downstream of the TGR (Fig. 7). The kaolinite contents tended to increase, while the chlorite contents showed a decreasing trend, and the illite contents increased first and then decreased along the water-flow direction. The montmorillonite content showed no spatial variations, however (Fig. 7). The elevation decreased gradually, and the climate gradually became warm and humid along the water-flow direction of the TGR; thus, kaolinite developed more significantly (Bainbridge et al. 2016; Liu et al. 2018).

Provenance of the TGR Sediments under Regular Dam Operation

Erosion rates were calculated to range between 0.18 and 0.6 mm/y for the upstream tributaries of the Yangtze River according to the depositional fluxes and concentrations of river sediments (Chappell et al. 2006; Godard et al. 2010; Kong et al. 2011; Vezzoli et al. 2016). The annual soil loss in the TGR was also estimated to be $1.57{\cdot}10^8$ t, of which $4{\cdot}10^7$ t entered the Yangtze River at the rate of 700 t km^{-2} y^{-1} (Liu et al. 2016a). In addition, the TGR tributaries produced large amounts of sediment inflows every year (Tang et al. 2016). In summary, the principal sediments supplied to the Three Gorges Reservoir could be divided into three groups with different sources based on their spatial scales: distal source (upstream tributaries such as Jinshajiang), regional source (TGR tributaries such as Xiangxihe), and proximal source (hillslope soil erosion in the TGR).

Among the distal sources, the clay-mineral compositions of Jinshajiang and Minjiang were closer to that of the TGR than those of the other three rivers (Yalongjiang, Daduhe, and Jialingjiang), especially Jinshajiang, which plotted in the center of the TGR field, while Minjiang was closer to the samples from the dry and even seasons (Fig. 8). All tributaries were generally close in clay-mineral compositions to the main stream sediments in the TGR. Values from the samples of the hillslope soils were scattered, and the hillslope soils contributed more to the sediments in the TGR during the flood season but less to the sediments in the other two seasons (Fig. 8). This was because frequent large rainfall events caused serious erosion of hillslope soils in the flood season. Large amounts of sediment were deposited in the TGR due to heavy

https://doi.org/10.1007/s42860-020-00106-5 Published online by Cambridge University Press

Table 1 Clay-mineral assemblages of the main stream, tributary sediments and the hillslope soils of the Three Gorges Reservoir

No.	Site	Season	Montmorillonite (%)	Illite (%)	Kaolinite (%)	Chlorite (%)	Illite chemistry index	Illite crystallinty (°Δ2θ)
1	M1	Flood season	5.6	68.3	9.6	16.6	0.43	0.53
2	M2		6.5	78.2	10.2	5.2	0.40	0.50
3	M3		2.4	79.8	11.3	6.6	0.49	0.50
4	M4		7.5	65.7	13.2	13.6	0.55	0.47
5	M5		4.2	70.6	11.9	13.3	0.46	0.52
6	M6		2.4	73.3	13.9	10.3	0.39	0.46
7	M7		3.3	66.8	16.9	13.0	0.48	0.49
8	M8		5.5	77.4	8.9	8.2	0.44	0.51
9	M1	Dry season	4.8	78.4	9.9	6.9	0.47	0.50
10	M2		5.0	71.1	14.5	9.5	0.42	0.49
11	M3		4.8	74.4	9.3	11.5	0.45	0.54
12	M4		0.6	80.1	10.5	8.9	0.51	0.54
13	M5		1.3	78.7	13.4	6.6	0.46	0.51
14	M6		5.3	70.4	15.4	9.0	0.43	0.57
15	M7		0.8	73.4	13.9	11.9	0.46	0.52
16	M8		0.5	78.3	12.4	8.9	0.44	0.48
17	M1	Even season	0.2	79.3	12.9	7.6	0.39	0.58
18	M2		3.8	72.7	13.5	10.1	0.40	0.54
19	M3		3.1	75.1	12.0	9.8	0.42	0.55
20	M4		4.0	77.1	14.4	4.6	0.34	0.60
21	M5		2.3	73.7	13.9	10.1	0.29	0.53
22	M6		0.6	80.6	11.4	7.4	0.44	0.52
23	M7		4.6	74.5	12.5	8.4	0.34	0.57
24	M8		1.8	74.4	14.3	9.5	0.33	0.44
25	Jiuwanxi	Flood season	10.2	71.2	11.7	6.9	0.45	0.48
26	Xiangxihe		9.4	58.0	16.3	16.4	0.34	0.52
27	Shennongxi		3.8	68.7	14.5	13.0	0.41	0.46
28	Daninghe		0.5	70.9	16.5	12.2	0.30	0.51
29	Meixihe		0.7	79.6	9.1	10.6	0.49	0.52
30	Changtanhe		3.2	77.9	8.6	10.2	0.25	0.50
31	Modaoxi		6.5	85.3	6.5	1.7	0.27	0.57
32	Tangxihe		4.3	76.7	10.7	8.2	0.58	0.47
33	Pengxihe		8.5	74.8	9.9	6.9	0.32	0.57
34	Jiuwanxi	Dry season	4.5	75.4	10.8	9.3	0.41	0.48
35	Xiangxihe		3.9	78.8	15.4	1.9	0.38	0.46
36	Shennongxi		0.6	73.8	12.7	13.0	0.43	0.47
37	Daninghe		0.4	80.6	10.2	8.8	0.38	0.51
38	Meixihe		0.4	84.3	12.0	3.3	0.46	0.54
39	Changtanhe		5.3	73.9	6.8	14.1	0.47	0.53
40	Modaoxi		3.6	73.8	16.4	6.2	0.39	0.53
41	Tangxihe		4.6	75.8	13.0	6.6	0.38	0.52
42	Pengxihe		7.8	74.4	11.0	6.8	0.28	0.65
43	Jiuwanxi	Even season	5.6	79.5	7.9	7.0	0.50	0.47
44	Xiangxihe		11.2	60.4	17.9	10.4	0.36	0.50
45	Shennongxi		0.8	78.5	10.0	10.7	0.46	0.48
46	Daninghe		6.1	72.6	7.4	13.9	0.40	0.49
47	Meixihe		1.7	83.4	8.3	6.7	0.33	0.63

https://doi.org/10.1007/s42860-020-00106-5 Published online by Cambridge University Press

Table 1 (continued)

No.	Site	Season	Montmorillonite (%)	Illite (%)	Kaolinite (%)	Chlorite (%)	Illite chemistry index	Illite crystallinty (°Δ2θ)
48	Changtanhe		4.4	75.2	6.6	13.8	0.46	0.55
49	Modaoxi		2.8	75.4	7.7	14.0	0.20	0.64
50	Tangxihe		5.8	76.0	4.2	14.3	0.36	0.58
51	Pengxihe		4.2	82.5	5.4	7.9	0.40	0.47
52	Longhe		5.7	77.1	8.0	9.2	0.49	0.50
53	Wujiang		6.0	72.7	11.0	10.2	0.31	0.54
54	S1		7.2	60.9	6.4	25.6	0.48	0.53
55	S2		7.2	59.5	8.7	24.5	0.35	0.64
56	S3		3.8	77.3	4.6	14.4	0.53	0.55
57	S4		11.5	72.9	5.5	10.1	0.18	0.33
58	S5		4.0	84.9	2.8	8.3	0.45	0.72
59	S6		5.0	79.7	4.1	11.2	0.27	0.66
60	S7		6.5	69.0	13.1	11.4	0.30	0.47
61	S8		2.1	67.7	11.6	18.6	0.33	0.44
62	S9		6.8	58.9	19.0	15.3	0.51	0.45
63	S10		4.0	68.6	14.4	13.0	0.37	0.45

rainfall (Bao et al. 2015, 2018). In summary, the distal sources, including Jinshajiang and Minjiang (in the dry and even seasons), and the TGR tributaries contributed much sediment to the TGR main stream, while the TGR hillslope soils made a greater contribution during the flood season than in the other two seasons.

Some major elements (Al, Fe, and Mg), other transition metals (e.g. Sc, Cr, and V), and high field strength elements are

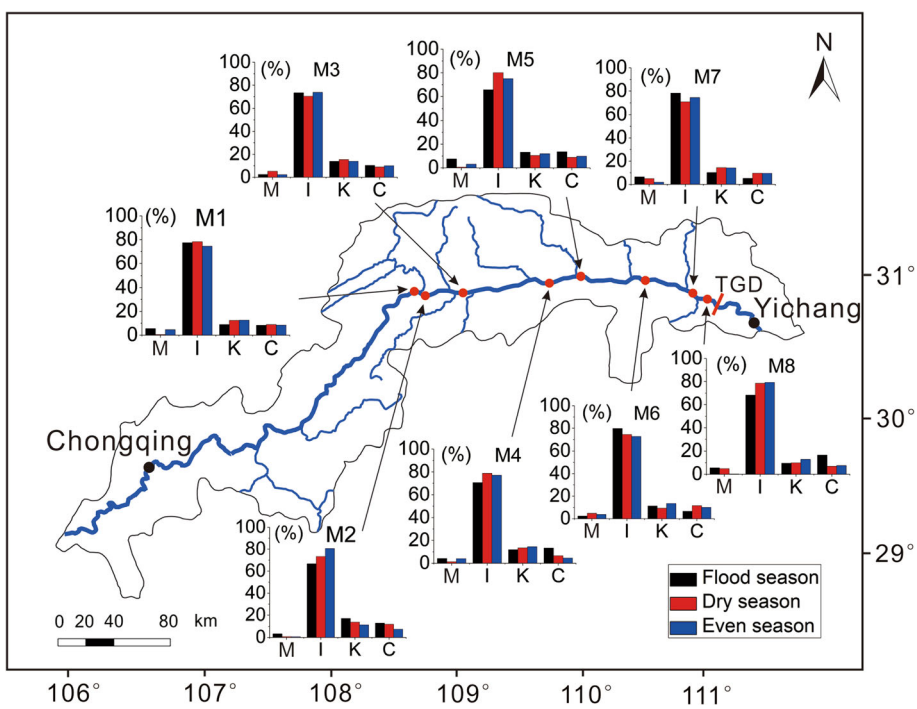

Fig. 5 Clay-mineral compositions in the main stream sediments of the TGR

https://doi.org/10.1007/s42860-020-00106-5 Published online by Cambridge University Press

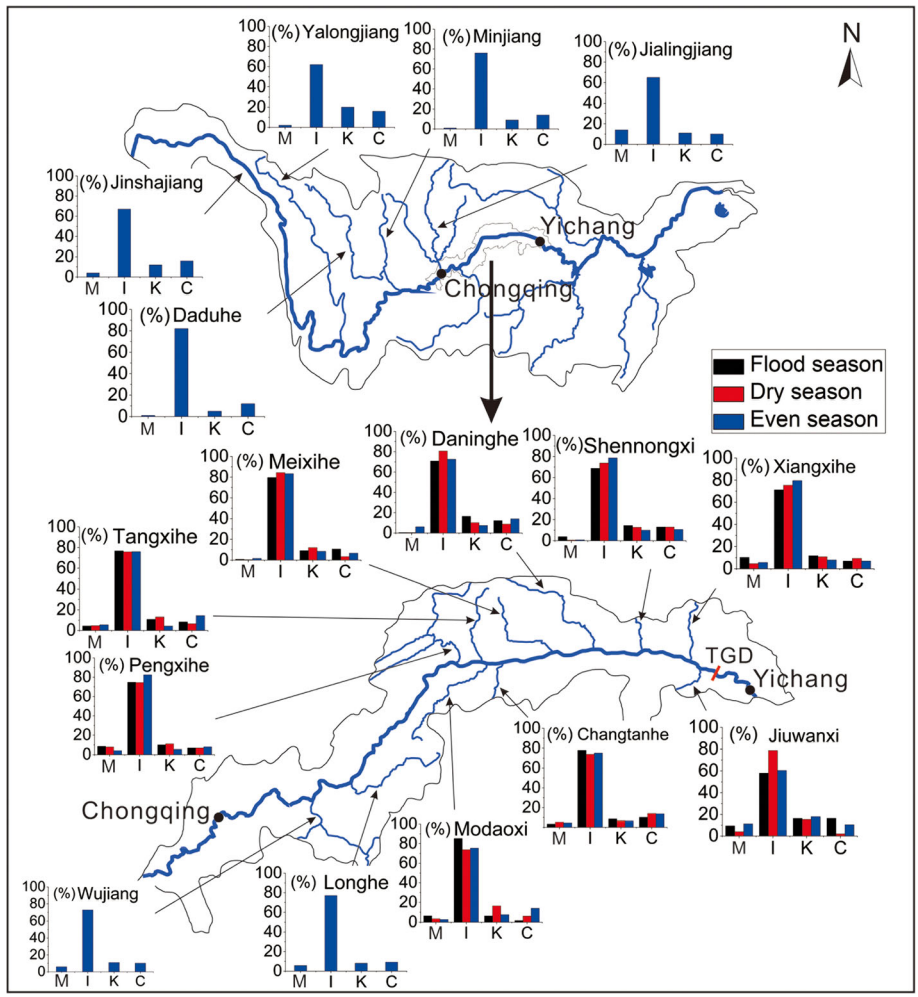

Fig. 6 Clay-mineral assemblages in the sediments of upstream tributaries and TGR tributaries. The data for Jinshajiang, Yalongjiang, Daduhe, Minjiang, and Jialingjiang are from He et al. (2013)

considered stable in a hypergene environment, and their ratios might represent the whole-rock composition of the source (Taylor and McLennan 1985). Therefore, pairs of these elemental ratios have been used widely to trace the provenance of sediments (Yang et al. 2004; Rao et al. 2015). The geochemical data of the distal source were summarized by He et al. (2015). From the elemental triangular diagrams (Fig. S3), geochemical similarities and differences between the TGR sediments and their potential sources could be observed more clearly. In general, TGR main stream sediments were constrained by each potential source, which indicated that TGR sediments were supplied by all three sources. Seasonally, the distal source contributed more to the TGR main stream sediments in the flood season than in the other two seasons. Spatially, the ternary diagrams of trace elements indicated that the distal source was the most important contributor, which was consistent with the results from clay minerals, while the major element ternary diagrams indicated that proximal and regional sources contributed more. Yang and Youn (2007) suggested that the fine fraction could not ultimately eliminate the grain-size effect, which influenced the provenance results from major elements. Nevertheless, the geochemical data supported the conclusions regarding clay minerals.

The annual sediment discharge of each source was summarized based on the hydrological data (Table 2) (CWRC 2003–2017; Yang et al. 2014; Liu et al. 2016a). The annual sediment discharge of the Jinsha River was greatest among the distal sources, and the annual sediment discharges from regional and proximal sources were also considerable (Table S2). The annual sediment discharge data from hydrological stations further supported the mineralogical results.

Implications for the Weathering Regime of River Sediments

Clay minerals in river sediments are good indicators of the weathering intensity across the watershed, and their compositions are controlled mainly by lithology, climate, structure, terrain environment, vegetation, and soil development (Mao et al. 2010; Bi et al. 2015; Wang et al. 2016). The clay-mineral compositions of river sediments varied widely in different

https://doi.org/10.1007/s42860-020-00106-5 Published online by Cambridge University Press

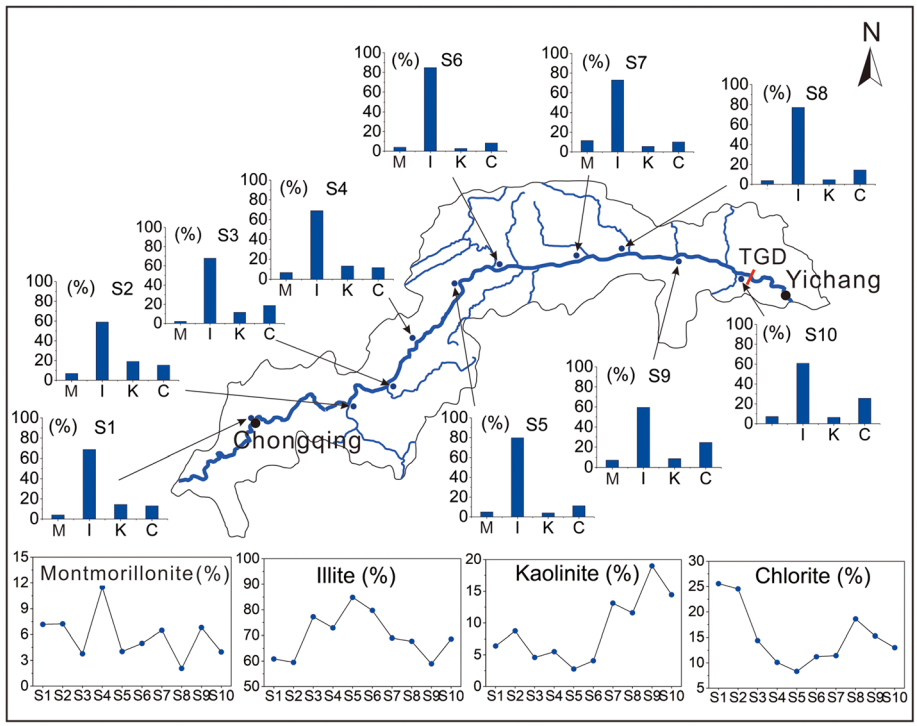

Fig. 7 Clay-mineral assemblages of the hillslope soils in the TGR

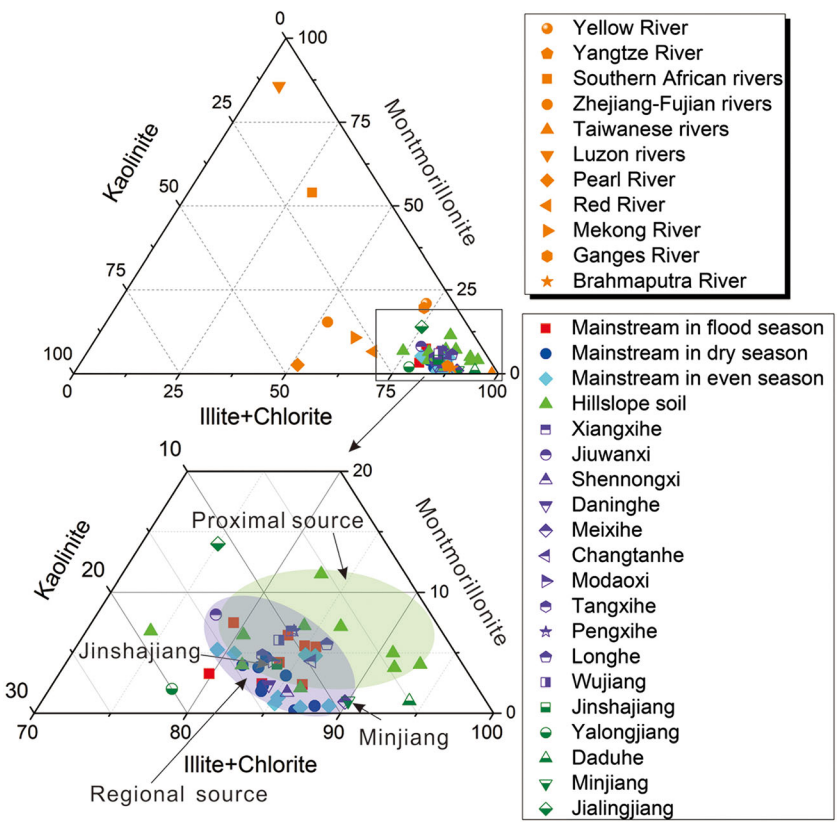

Fig. 8 Ternary diagram of the major clay-mineral groups: illite + chlorite, kaolinite, and montmorillonite in the TGR and rivers worldwide

https://doi.org/10.1007/s42860-020-00106-5 Published online by Cambridge University Press

Table 2 Average concentration of major and trace elements of sediments and hillslope soil in the Three Gorges Reservoir

Elements	Main stream						Tributaries						Hillslope soil	
	Flood season (*n*=3)		Dry season (*n*=3)		Even season (*n*=3)		Flood season (*n*=3)		Dry season (*n*=3)		Even season (*n*=3)		(*n*=3)	
	Mean	Std.	Mean	Std.	Mean	Std.	Mean	Std.	Mean	Std.	Mean	Std.	Mean	Std.
Al_2O_3 (%)	18.86	1.39	19.89	1.38	17.83	1.27	16.74	1.82	17.83	0.83	17.03	0.96	18.05	1.32
CaO	1.20	0.03	1.04	0.2	1.48	0.24	2.26	2.44	0.85	0.22	1.8	0.95	1.11	0.03
Fe_2O_3	8.49	0.63	8.27	0.3	8.57	0.18	6.95	0.37	6.64	0.69	6.49	0.59	7.20	0.88
K_2O	3.52	0.28	3.78	0.29	3.37	0.19	3.5	0.33	3.4	0.34	3.38	0.24	3.37	0.25
MgO	2.72	0.31	2.94	0.14	2.89	0.11	3.5	1.21	2.46	0.74	2.65	0.53	2.77	0.28
MnO	0.13	0.03	0.12	0.01	0.13	0.02	0.11	0.01	0.1	0	0.1	0.01	0.11	0.01
Na_2O	0.78	0.12	0.71	0.12	0.83	0.09	0.63	0.22	0.9	0.25	0.81	0.33	1.06	0.20
P_2O_5	0.23	0.02	0.22	0.02	0.24	0.01	0.42	0.29	0.19	0.03	0.16	0.02	0.20	0.02
TiO_2	0.97	0.03	1	0.05	1.15	0.12	0.86	0.05	0.88	0.02	0.86	0.06	0.99	0.13
SiO_2	58.71	2.85	57.99	1.94	58.88	1.26	59.43	4.14	62.78	3.04	61.93	2.96	60.69	3.24
Li (μg/g)	61.63	6.67	75.56	16.18	67.46	22.45	75.05	22.03	76.93	10.57	78.81	10.57	80.10	11.84
Be	3.04	0.19	3.44	0.55	3.46	1.22	2.68	0.35	3.38	0.28	3.75	0.28	3.48	0.44
Rb	146.86	11.03	150.72	29.23	126.8	43.6	129.88	18.61	144.78	10.27	152.52	10.27	145.87	26.49
Sr	102.22	2.65	108.78	4.06	93.56	34.45	85.14	20.1	95.01	5.09	124.78	5.09	105.11	8.91
Ba	583.16	21.37	627.41	63.05	537.92	200.44	668.76	160.31	630.48	16.68	722.45	16.68	484.40	53.06
V	134.25	10.19	154.62	22.18	128.39	44.64	138.43	29.55	134.71	10.81	129.71	10.81	129.79	19.18
Cr	106.96	6.17	116.89	17.09	98.29	34.25	97.33	3.4	98.63	8.04	106.25	8.04	98.46	8.87
Co	20.27	1.67	21.85	2.94	18.38	6.21	17.33	0.41	18.13	0.66	19.78	0.66	16.76	4.51
Ni	51.57	3.45	56.21	7.65	47.58	16.41	50.12	3.83	48.21	4.64	49.64	4.64	44.79	5.19
Cu	53.12	3.44	66.59	7.15	59.09	24.2	39.73	0.97	42.95	3.45	37.8	3.45	39.05	13.90
Zn	322.52	232.72	176.65	30.84	155.5	51.26	130.1	14.74	122.14	8.49	126.21	8.49	116.42	30.78
Sc	16.83	0.97	18.37	2.77	15.4	5.4	15.16	1.5	16.57	1.43	17.05	1.43	17.02	2.27
Y	22.76	0.44	23.4	2.46	19.69	6.89	21.28	1.03	22.52	1.02	24.76	1.02	26.51	4.89
Zr	127.30	2.80	136.2	14.71	114.52	42.99	117.75	8.75	141.89	3.01	154.51	3.01	159.73	38.81
Nb	16.30	0.63	17.66	1.71	15.16	5.54	14.48	0.86	16.47	0.88	17.66	0.88	19.37	4.47
Hf	3.54	0.05	3.72	0.43	3.01	1.11	3.26	0.27	3.84	0.15	4.1	0.15	4.32	1.10
Ta	1.60	0.78	3.97	4.89	1.06	0.39	1.03	0.08	1.15	0.7	1.87	0.7	3.31	3.57
Pb	66.20	11.95	62.55	6.86	55.34	16.26	31.13	4.79	33.8	0.69	34.57	0.69	28.00	5.05
Th	14.34	0.40	14.1	2.32	11.81	3.98	12.61	0.67	13.51	0.34	14.37	0.34	16.49	2.72
U	2.85	0.18	2.96	0.5	2.48	0.85	2.96	0.27	3.04	0.1	3.12	0.1	3.38	0.77

regions (Fig. 8 and Table S3). Rivers such as the Yangtze River (including the TGR area) that originated from plateaus or tall mountains were dominated by illite (Table S3). These observations implied that illite was a residue produced by the physical decomposition of micas in metamorphic rocks or of feldspar to sericite (Garzanti et al. 2014). Compared with the Yangtze River as a whole, however, the TGR contained sediments that showed mainly significant illite crystallinity and low illite chemical index, which indicated that the sediments were subjected to significant physical weathering and to weak hydrolysis of rocks (Fig. 9). These processes occurred mainly because the upstream lithologies in the Yangtze River, as the main source of sediments in the TGR, were subjected mainly to physical weathering in cold-arid climates (Zhao et al. 2018). The TGR sediments showed seasonal variations. The chemical index of TGR sediments was higher in the flood season than in the dry and even seasons (Fig. 9). Moreover, the chemical index of sediments in the flood season was >0.4, which meant that the sediment contained Al-rich illite and had experienced intense hydrolysis, but the sediments in the other two seasons had Fe- and Mg-rich illite, resulting from physical weathering (Chamley 1989; Liu et al. 2008; He et al. 2013). Throughout the whole Yangtze River Basin, the disparities in illite indices between the northern and southern tributaries were remarkable (Fig. 9). Northern tributaries of the Yangtze River had greater illite and smaller kaolinite abundances than those of southern tributaries, which reflected the differences in their climates and weathering environments. The southern tributaries had a

https://doi.org/10.1007/s42860-020-00106-5 Published online by Cambridge University Press

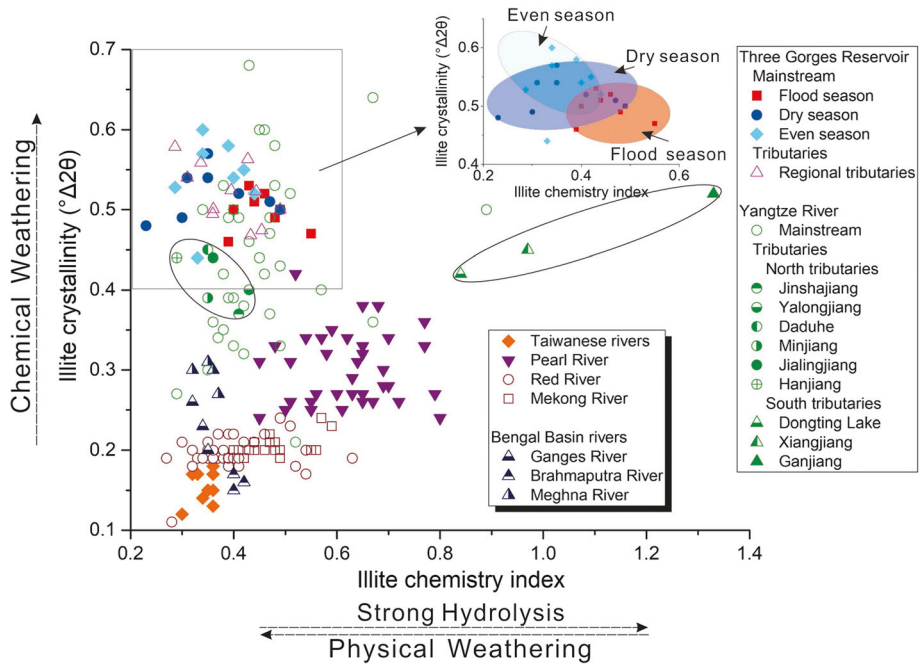

Fig. 9 Correlation between the illite chemistry index and the illite crystallinity of the sediments in the TGR and other rivers

relatively warmer and more humid climate together with stable morphology and low relief (He et al. 2013).

In sharp contrast, the montmorillonite contents in rivers (Luzon and Ganges Rivers) from the tropics and subtropics were very large (Fig. 8 and Table S3). This occurred because the formation of montmorillonite requires a warm climate with the rainy season separated from the dry season with strong evaporation (Velde 1995; Liu et al. 2010; He et al. 2013). The long-lasting and intense hydrolysis due to the low-relief and stable morphology caused greater kaolinite abundances in the Pearl, Mekong, Zhejiang, and Fujian Rivers (Liu et al. 2007, 2016b; Khan et al. 2019). Meanwhile, the Taiwanese rivers,

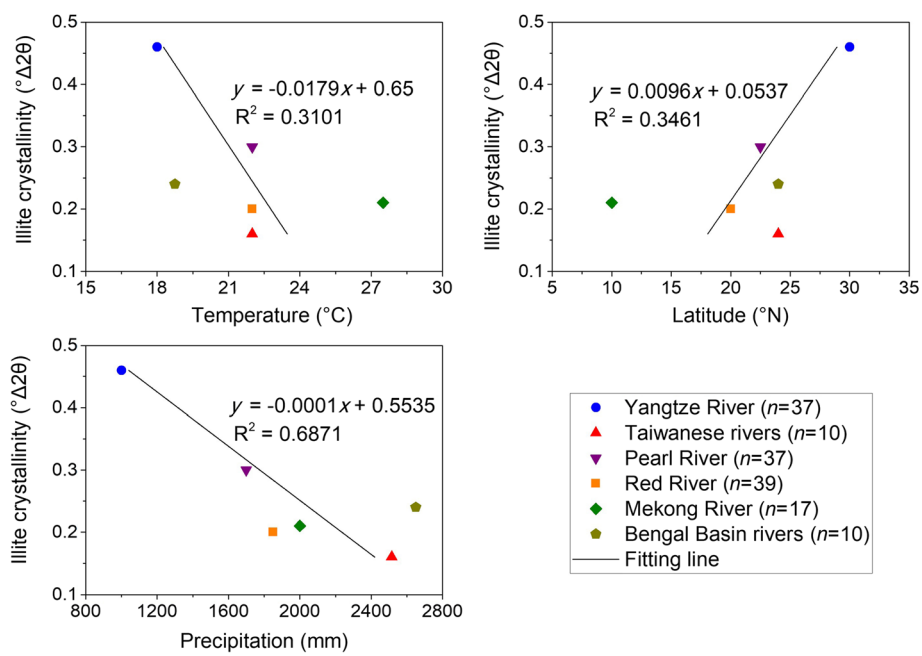

Fig. 10 Diagrams of illite crystallinity vs. temperature, latitude, and precipitation in the TGR sediments. The data f temperature, latitude, and precipitation were from He et al. (2013) for the Yangtze River, from Li et al. (2012) for the Taiwanese rivers, from Liu et al. (2007) for the Pearl, Red, and Mekong Rivers, and from Khan et al. (2019) for the Bengal Basin rivers

https://doi.org/10.1007/s42860-020-00106-5 Published online by Cambridge University Press

the Red river, the Mekong River, the Pearl River, and the Bengal Basin Rivers are situated at lower latitudes than the Yangtze River (including the TGR area). They are located at similar latitudes and are influenced by typhoons and monsoon cycles with warm and humid weather systems, which cause the illite indices of these river sediments to fall within a relatively small range (Fig. 9). More intense chemical weathering in the Pearl River, however, was attested by higher illite indices than those in the other rivers (Liu et al. 2007). The Bengal Basin rivers sediments were formed by physical weathering processes because of the small illite chemical index values (<0.4) (Khan et al. 2019). The sediments in Taiwanese rivers had much lower FWHM values than other Asian rivers, which reflected strong physical erosion (Wang et al. 2016).

Some scholars have suggested that weathering intensity may be affected by climate and geographical location (Wang et al. 2016; Khan et al. 2019). The relationships between the meteorological parameters (precipitation and temperature), latitude, and illite crystallinity in the Asian rivers were explored. As shown in Fig. 10, the influences of latitude and temperature on the illite crystallinity were small, while precipitation had a significant effect on illite crystallinity; i.e. the greater the annual precipitation, the stronger the chemical weathering effect. In summary, precipitation was the dominant factor affecting the weathering intensity.

CONCLUSIONS

The clay mineralogy and geochemistry of main stream and tributary sediments and hillslope soils collected from the Three Gorges Reservoir (TGR) Basin, China, were investigated to identify sediment provenances and weathering regimes.

The results indicated that common minerals were dominated by quartz, followed by clay minerals, plagioclase, and K-feldspar in the TGR sediments and hillslope soils. Illite, kaolinite, chlorite, and montmorillonite were identified using SEM. Clay-mineral compositions throughout the TGR were dominated by illite, with less kaolinite and chlorite, and scarce montmorillonite. The amounts of illite and kaolinite in the flood season were slightly smaller than those in the dry and even seasons, but the amounts of chlorite and montmorillonite in the flood season were slightly greater than in the other two seasons. Large amounts of SiO_2 and Al_2O_3 and small amounts of other elements were distinctive features of TGR sediments and soils, while the mean elemental concentrations did not differ greatly among the three seasons for the TGR sediments.

Three major sources of sediments were distinguished in the TGR. Based on the analysis of mineralogical, geochemical, and hydrological data, the distal sources, including Jinshajiang and Minjiang (in the dry and even seasons), contributed much sediment to the TGR. The regional source, which includes all the TGR tributaries, was also a main contributor during the flood, dry, and even seasons, and the proximal source, hillslope soils, contributed more in the flood season than in the other two seasons.

Compared to the whole Yangtze River, the TGR contained sediments that had high illite crystallinity and a low illite chemical index, reflecting strong physical weathering and weak hydrolysis of rocks. The chemical indices of sediments during the flood season in the TGR were mostly >0.4, which meant that the sediments consisted of Al-rich illite and had experienced intense hydrolysis, but the sediments during the other two seasons consisted of Fe- and Mg-rich illite resulting from physical weathering. In addition, chemical weathering was affected mainly by precipitation, while temperature and latitude had less influence.

SUPPLEMENTARY INFORMATION

The online version contains supplementary material available at https://doi.org/10.1007/s42860-020-00106-5.

ACKNOWLEDGMENTS

This study was supported financially by the National Key Research and Development Program of China (Grant No. 2016YFC0401703), the Fundamental Research Funds for the Central Universities (B200203111), the Natural Science Foundation of Jiangsu Province (Grant No. BK20191304), the Fundamental Research Funds for the Central Universities (Grant No. 2019B45414), the Postgraduate Research & Practice Innovation Program of Jiangsu Province (KYCX20_0490), and China Scholarship Council (CSC). Dr Tianning Li and Xiaofan Ma are acknowledged for help with the experiments.

Funding

Funding sources are as stated in the Acknowledgments.

Compliance with Ethical Statements

Conflict of Interest

The authors declare that they have no conflict of interest.

REFERENCES

Adriaens, R., Zeelmaekers, E., Fettweis, M., Vanlierde, E., Vanlede, J., Stassen, P., Elsen, J., Środoń, J., & Vandenberghe, N. (2018). Quantitative clay mineralogy as provenance indicator for recent muds in the southern North Sea. *Marine Geology, 398*, 48–58. https://doi.org/10.1016/j.margeo.2017.12.011.

Bainbridge, Z., Lewis, S., Smithers, S., Wilkinson, S., Douglas, G., Hillier, S., & Brodie, J. (2016). Clay mineral source tracing and characterisation of Burdekin River (NE Australia) and flood plume fine sediment. *Journal of Soils and Sediments, 16*, 687–706. https://doi.org/10.1007/s11368-015-1282-4.

Bao, Y., Gao, P., & He, X. (2015). The water-level fluctuation zone of Three Gorges Reservoir – A unique geomorphological unit. *Earth-Science Reviews, 150*, 14–24. https://doi.org/10.1016/j.earscirev.2015.07.005.

Bao, Y., He, X., Wen, A., Gao, P., Tang, Q., Yan, D., & Long, Y. (2018). Dynamic changes of soil erosion in a typical disturbance zone of China's Three Gorges Reservoir. *Catena, 169*, 128–139. https://doi.org/10.1016/J.CATENA.2018.05.032.

Bi, L., Yang, S., Li, C., Guo, Y., Wang, Q., Liu, J. T., & Yin, P. (2015). Geochemistry of river-borne clays entering the East China Sea indicates two contrasting types of weathering and sediment transport processes. *Geochemistry, Geophysics, Geosystems, 16*, 3034–3052.

Biscaye, P. E. (1965). Mineralogy and sedimentation of recent deep-sea clay in the Atlantic Ocean and adjacent seas and oceans. *Geological Society of America Bulletin, 76*, 803–832.

Chamley, H. (1989). *Clay Sedimentology* (pp. 1–623). Berlin: Springer.

Chappell, J., Zheng, H., & Fifield, K. (2006). Yangtse River sediments and erosion rates from source to sink traced with cosmogenic 10Be: Sediments from major rivers. *Palaeogeography, Palaeoclimatology, Palaeoecology, 241*, 79–94. https://doi.org/10.1016/j.palaeo.2006.06.010.

Chen, X., Yan, Y., Fu, R., Dou, X., & Zhang, E. (2008). Sediment transport from the Yangtze River, China, into the sea over the Post-Three Gorge Dam Period: A discussion. *Quaternary International, 186*, 55–64. https://doi.org/10.1016/j.quaint.2007.10.003.

CNEMC (China National Environmental Monitoring Centre) (1997–2017). Bulletin of ecological and environmental monitoring of the Three Gorges Project in the Yangtze River. PR China: Ministry of Environment Protection. (*in Chinese*)

Cook, H. E., Johnson, P. D., Matti, J. C., & Zemmels, I. (1975). Methods of Sample Preparation and X-Ray Diffraction Data Analysis, X-Ray Minerology Laboratory, Deep Sea Drilling Project, University of California, Riverside. *Initial Reports of the DSDP, 28*, 999–1007.

CWRC (Changjiang Water Resource Commission) (2003–2017). Changjiang Sediment Bulletin. Wuhan: Changjiang Press (*in Chinese*).

Ehrmann, W. (1998). Implications of late Eocene to early Miocene clay mineral assemblages in McMurdo sound (Ross Sea, Antarctica) on paleoclimate and ice dynamics. *Palaeogeography, Palaeoclimatology, Palaeoecology, 139*, 213–231. https://doi.org/10.1016/S0031-0182(97)00138-7.

Fu, B. J., Wu, B. F., Lü, Y. H., Xu, Z. H., Cao, J. H., Niu, D., Yang, G. S., & Zhou, Y. M. (2010). Three Gorges Project: Efforts and challenges for the environment. *Progress in Physical Geography, 34*, 741–754. https://doi.org/10.1177/0309133310370286.

Garzanti, E., Padoan, M., Setti, M., López-Galindo, A., & Villa, I. M. (2014). Provenance versus weathering control on the composition of tropical river mud (southern Africa). *Chemical Geology, 366*, 61–74. https://doi.org/10.1016/j.chemgeo.2013.12.016.

Gingele, F. X., De Deckker, P., & Hillenbrand, C. D. (2001). Clay mineral distribution in surface sediments between Indonesia and NW Australia – Source and transport by ocean currents. *Marine Geology, 179*, 135–146. https://doi.org/10.1016/S0025-3227(01)00194-3.

Godard, V., Lavé, J., Carcaillet, J., Cattin, R., Bourlès, D., & Zhu, J. (2010). Spatial distribution of denudation in Eastern Tibet and regressive erosion of plateau margins. *Tectonophysics, 491*, 253–274. https://doi.org/10.1016/j.tecto.2009.10.026.

Gürel, A. (2017). Geology, mineralogy, and geochemistry of late Miocene paleosol and calcrete in the western part of the Central Anatolian Volcanic Province. *Geoderma, 302*, 22–38. https://doi.org/10.1016/j.geoderma.2017.04.016.

Gürel, A., & Özcan, S. (2016). Paleosol and dolocrete associated clay mineral occurrences in siliciclastic red sediments of the Late Miocene Kömişini Formation of the Tuzgölü basin in central Turkey. *Catena, 143*, 102–113. https://doi.org/10.1016/j.catena.2016.04.003.

Guyot, J. L., Jouanneau, J. M., Soares, L., Boaventura, G. R., Maillet, N., & Lagane, C. (2007). Clay mineral composition of river sediments in the Amazon Basin. *Catena, 71*, 340–356. https://doi.org/10.1016/j.catena.2007.02.002.

He, M., Zheng, H., Huang, X., Jia, J., & Li, L. (2013). Yangtze River sediments from source to sink traced with clay mineralogy. *Journal of Asian Earth Sciences, 69*, 60–69. https://doi.org/10.1016/j.jseaes.2012.10.001.

He, M., Zheng, H., Clift, P. D., Tada, R., Wu, W., & Luo, C. (2015). Geochemistry of fine-grained sediments in the Yangtze River and the implications for provenance and chemical weathering in East Asia. *Progress in Earth and Planetary Science, 2*, 32. https://doi.org/10.1186/s40645-015-0061-6.

Huang, Y., Wang, J., & Yang, M. (2019). Unexpected sedimentation patterns upstream and downstream of the Three Gorges Reservoir: Future risks. *International Journal of Sediment Research, 34*, 108–117. https://doi.org/10.1016/j.ijsrc.2018.05.004.

Khan, M. H. R., Liu, J., Liu, S., Seddique, A. A., Cao, L., & Rahman, A. (2019). Clay mineral compositions in surface sediments of the Ganges-Brahmaputra-Meghna river system of Bengal Basin, Bangladesh. *Marine Geology, 412*, 27–36. https://doi.org/10.1016/j.margeo.2019.03.007.

Kong, P., Zheng, Y., & Fu, B. (2011). Cosmogenic nuclide burial ages and provenance of Late Cenozoic deposits in the Sichuan Basin: Implications for Early Quaternary glaciations in east Tibet. *Quaternary Geochronology, 6*, 304–312. https://doi.org/10.1016/j.quageo.2011.03.006.

Li, Q., Yu, M., Lu, G., Cai, T., Bai, X., & Xia, Z. (2011). Impacts of the Gezhouba and Three Gorges Reservoirs on the sediment regime in the Yangtze River, China. *Journal of Hydrology, 403*, 224–233. https://doi.org/10.1016/j.jhydrol.2011.03.043.

Li, C. S., Shi, X. F., Kao, S. J., Te Chen, M., Liu, Y. G., Fang, X. S., Lü, H. H., Zou, J. J., Liu, S. F., & Qiao, S. Q. (2012). Clay mineral composition and their sources for the fluvial sediments of Taiwanese rivers. *Chinese Science Bulletin, 57*, 673–681. https://doi.org/10.1007/s11434-011-4824-1.

Liu, Z., Trentesaux, A., Clemens, S. C., Colin, C., Wang, P., Huang, B., & Boulay, S. (2003). Clay mineral assemblages in the northern South China Sea: Implications for East Asian monsoon evolution over the past 2 million years. *Marine Geology, 201*, 133–146. https://doi.org/10.1016/S0025-3227(03)00213-5.

Liu, Z., Colin, C., Huang, W., Phon Le, K., Tong, S., Chen, Z., & Trentesaux, A. (2007). Climatic and tectonic controls on weathering in south China and Indochina Peninsula: Clay mineralogical and geochemical investigations from the Pearl, Red, and Mekong drainage basins. *Geochemistry, Geophysics, Geosystems, 8*, 1–18. https://doi.org/10.1029/2006GC001490.

Liu, Z., Tuo, S., Colin, C., Liu, J. T., Huang, C. Y., Selvaraj, K., Chen, C., Zhao, Y., Siringan, F., Boulay, S., & Chen, Z. (2008). Detrital fine-grained sediment contribution from Taiwan to the northern South China Sea and its relation to regional ocean circulation. *Marine Geology, 255*, 149–155. https://doi.org/10.1016/j.margeo.2008.08.003.

Liu, Z., Colin, C., Li, X., Zhao, Y., Tuo, S., Chen, Z., Siringan, F., Liu, J., Huang, C., You, C., & Huang, K. F. (2010). Clay mineral distribution in surface sediments of the northeastern South China Sea and surrounding fluvial drainage basins: Source and transport. *Marine Geology, 277*, 48–60. https://doi.org/10.1016/j.margeo.2010.08.010.

Liu, G., Xiao, H., Liu, P., Zhang, Q., & Zhang, J. (2016a). Using rare earth elements to monitor sediment sources from a miniature model of a small watershed in the Three Gorges area of China. *Catena, 143*, 114–122. https://doi.org/10.1016/j.catena.2016.03.044.

Liu, Z., Zhao, Y., Colin, C., Stattegger, K., Wiesner, M. G., Huh, C. A., Zhang, Y., Li, X., Sompongchaiyakul, P., You, C., Huang, C., Liu, J., Siringan, F., Le, K., Sathiamurthy, E., Hantoro, W., Liu, J., Tuo, S., Zhao, S., Zhou, Z., He, Z., Wang, Y., Bunsomboonsakul, S., & Li, Y. (2016b). Source-to-sink transport processes of fluvial sediments in the South China Sea. *Earth-Science Reviews, 153*, 238–273. https://doi.org/10.1016/j.earscirev.2015.08.005.

Liu, J., Cao, K., Yin, P., Gao, F., Chen, X., Zhang, Y., & Yu, Y. (2018). The Sources and Transport Patterns of Modern Sediments in Hangzhou Bay: Evidence from Clay Minerals. *Journal of Ocean University of China, 17*, 1352–1360. https://doi.org/10.1007/s11802-018-3710-8.

Lou, B., & Yin, S. (2016). Spatial and seasonal distribution of phosphorus in the mainstem within the Three Gorges Reservoir before and after impoundment. *Water Science and Technology, 73*, 636–642. https://doi.org/10.2166/wst.2015.516.

Lu, X. X., & Higgitt, D. L. (2001). Sediment delivery to the Three Gorges 2: Local response. *Geomorphology, 41*, 157–169. https://doi.org/10.1016/S0169-555X(01)00113-1.

Mao, C., Chen, J., Yuan, X., Yang, Z., Balsam, W., & Ji, J. (2010). Seasonal variation in the mineralogy of the suspended particulate matter of the lower Changjiang river at Nanjing, China. *Clays and Clay Minerals, 58*, 691–706. https://doi.org/10.1346/CCMN.2010.0580508.

Pang, H., Pan, B., Garzanti, E., Gao, H., Zhao, X., & Chen, D. (2018). Mineralogy and geochemistry of modern Yellow River sediments: Implications for weathering and provenance. *Chemical Geology, 488*, 76–86. https://doi.org/10.1016/j.chemgeo.2018.04.010.

Rao, W., Tan, H., Chen, J., Ji, J., Chen, Y., Pan, Y., & Zhang, W. (2015). Nd–Sr isotope geochemistry of fine-grained sands in the basin-type deserts, West China: Implications for the source mechanism and atmospheric transport. *Geomorphology, 246*, 458–471. https://doi.org/10.1016/j.geomorph.2015.06.043.

Tang, Q., Bao, Y., He, X., Fu, B., Collins, A. L., & Zhang, X. (2016). Flow regulation manipulates contemporary seasonal sedimentary dynamics in the reservoir fluctuation zone of the Three Gorges Reservoir, China. *Science of the Total Environment, 548–549*, 410–420. https://doi.org/10.1016/j.scitotenv.2015.12.158.

Taylor, S. R., & McLennan, S. M. (1985). *The Continental Crust: Its Composition and Evolution*. Oxford: Blackwell.

Vanderaveroet, P. (2000). Miocene to Pleistocene clay mineral sedimentation on the New Jersey shelf. *Oceanologica Acta, 23*, 25–36. https://doi.org/10.1016/S0399-1784(00)00102-X.

Velde, B. (1995). *Origin and Mineralogy of Clays*. Berlin: Springer 371 pp.

Vezzoli, G., Garzanti, E., Limonta, M., Andò, S., & Yang, S. (2016). Erosion patterns in the Changjiang (Yangtze River) catchment revealed by bulk-sample versus single-mineral provenance budgets. *Geomorphology, 261*, 177–192. https://doi.org/10.1016/j.geomorph.2016.02.031.

Wang, Y., Fan, D., Liu, J. T., & Chang, Y. (2016). Clay-mineral compositions of sediments in the Gaoping River-Sea system: Implications for weathering, sedimentary routing and carbon cycling. *Chemical Geology, 447*, 11–26. https://doi.org/10.1016/j.chemgeo.2016.10.024.

Wang, K., Li, Z. X., Dong, S., Cui, J., Han, B., Zheng, T., & Xu, Y. (2018). Early crustal evolution of the Yangtze Craton, South China: New constraints from zircon U-Pb-Hf isotopes and geochemistry of ca. 2.9–2.6 Ga granitic rocks in the Zhongxiang Complex. *Precambrian Research, 314*, 325–352. https://doi.org/10.1016/j.precamres.2018.05.016.

Winkler, A., Wolf-Welling, T., Stattegger, K., & Thiede, J. (2002). Clay mineral sedimentation in high Northern latitude deep-sea basins since the Middle Miocene (ODP Leg 151, NAAG). *International Journal of Earth Sciences, 91*, 133–148. https://doi.org/10.1007/s005310100199.

Wu, J., Huang, J., Han, X., Xie, Z., & Gao, X. (2003). Three-Gorge dam-experiment in habitat fragmentation. *Science, 300*, 1239–1240.

Xu, K., Milliman, J. D., & Xu, H. (2010). Temporal trend of precipitation and runoff in major Chinese Rivers since 1951. *Global and Planetary Change, 73*, 219–232. https://doi.org/10.1016/j.gloplacha.2010.07.002.

Xu, X., Tan, Y., & Yang, G. (2013a). Environmental impact assessments of the Three Gorges Project in China: Issues and interventions. *Earth-Science Reviews, 124*, 115–125. https://doi.org/10.1016/j.earscirev.2013.05.007.

Yang, S. L., & Youn, J. S. (2007). Geochemical compositions and provenance discrimination of the central south Yellow Sea sediments. *Marine Geology, 243*, 229–241. https://doi.org/10.1016/j.margeo.2007.05.001.

Yang, S. L., Zhao, Q. Y., & Belkin, I. M. (2002). Temporal variation in the sediment load of the Yangtze river and the influences of human activities. *Journal of Hydrology, 263*, 56–71. https://doi.org/10.1016/S0022-1694(02)00028-8.

Yang, S. Y., Lim, D. I., Jung, H. S., & Oh, B. C. (2004). Geochemical composition and provenance discrimination of coastal sediments around Cheju Island in the southeastern Yellow Sea. *Marine Geology, 206*, 41–53. https://doi.org/10.1016/j.margeo.2004.01.005.

Yang, S. L., Zhang, J., & Xu, X. J. (2007). Influence of the Three Gorges Dam on downstream delivery of sediment and its environmental implications, Yangtze River. *Geophysical Research Letters, 34*, 1–5. https://doi.org/10.1029/2007GL029472.

Yang, S., Wang, Z., Guo, Y., Li, C., & Cai, J. (2009). Heavy mineral compositions of the Changjiang (Yangtze River) sediments and their provenance-tracing implication. *Journal of Asian Earth Sciences, 35*, 56–65. https://doi.org/10.1016/j.jseaes.2008.12.002.

Yang, S. L., Milliman, J. D., Xu, K. H., Deng, B., Zhang, X. Y., & Luo, X. X. (2014). Downstream sedimentary and geomorphic impacts of the Three Gorges Dam on the Yangtze River. *Earth-Science Reviews, 138*, 469–486. https://doi.org/10.1016/j.earscirev.2014.07.006.

Zhang, Q., & Lou, Z. (2011). The environmental changes and mitigation actions in the Three Gorges Reservoir region, China. *Environmental Science and Policy, 14*, 1132–1138. https://doi.org/10.1016/j.envsci.2011.07.008.

Zhao, Y., Zou, X., Gao, J., Wang, C., Li, Y., Yao, Y., Zhao, W., & Xu, M. (2018). Clay mineralogy and source-to-sink transport processes of Changjiang River sediments in the estuarine and inner shelf areas of the East China Sea. *Journal of Asian Earth Sciences, 152*, 91–102. https://doi.org/10.1016/j.jseaes.2017.11.038.

Zhou, C. H., Zhao, L. Z., Wang, A. Q., Chen, T. H., & He, H. P. (2016). Current fundamental and applied research into clay minerals in China. *Applied Clay Science, 119*, 3–7. https://doi.org/10.1016/j.clay.2015.07.043.

(Received 22 May 2020; revised 13 November 2020; AE: Selahattin Kadir)